Chapter 6
Intrusions of the Kulumbe River Valley, NW Siberian Traps Province: Paleomagnetism, Magnetic Fabric and Geochemistry

A. V. Latyshev, N. A. Krivolutskaya, P. S. Ulyahina, Ya. V. Bychkova and B. I. Gongalsky

Abstract We present the new geochemical, paleomagnetic and anisotropy of magnetic susceptibility data from the Kulumbe river area (the Siberian Traps Large Igneous Province). The majority of the studied intrusions have the normal polarity, belong to the Katangsky complex and can be correlated with the upper part of the volcanic section of the Norilsk region. Furthermore, the first intrusive analogues of the Gudchikhinsky Formation are found. The only intrusion showing the reverse magnetic polarity has the geochemical features similar to the ore-bearing Norilsk-type intrusions. Based on the study of the magnetic fabric of the intrusions, we suggest that they were fed from the magma-conducting Imangda-Letninskiy fault.

Keywords Paleomagnetism · Geochemistry · Siberian traps · Anisotropy of magnetic susceptibility · Cu-Ni-PGE deposits

A. V. Latyshev (✉) · P. S. Ulyahina · Ya. V. Bychkova
Geological Faculty, Lomonosov Moscow State University, Moscow, Russia
e-mail: anton.latyshev@gmail.com

A. V. Latyshev · P. S. Ulyahina
Schmidt Institute, Physics of the Earth, Russian Academy of Sciences, Moscow, Russia

N. A. Krivolutskaya
Vernadsky Institute of Geochemistry and Analytical Chemistry, Russian Academy of Sciences, Moscow, Russia

B. I. Gongalsky
Institute Geology of Ore Deposits, Petrography, Mineralogy and Geochemistry, Russian Academy of Sciences, Moscow, Russia

D. Nurgaliev et al. (eds.), *Recent Advances in Rock Magnetism, Environmental Magnetism and Paleomagnetism*, Springer Geophysics,
https://doi.org/10.1007/978-3-319-90437-5_6

Introduction

The problem of the origin of Large Igneous Provinces (LIPs) and associated mineralization is one of the major open questions in geology (Dobretsov 1997; Ernst 2014). The Siberian Traps contain the world-class PGE-Cu-Ni Norilsk deposits, which are the only example of the unique ores within a young (~251 Ma, Kamo et al. 2003; Burgess and Bowring 2015) large igneous province, while the bulk of similar deposits is related to large Proterozoic basic-ultrabasic plutons. Mineralization is associated with the Permian-Triassic sill-like intrusions of the NW part of the Siberian platform while cognate intrusive bodies are widespread around the trap province. Therefore, the question of the place of the Norilsk ore-bearing intrusions in the LIP evolution has both fundamental scientific and applied importance. In particular, it directly contributes to the successful prospecting of the new deposits not only within the Siberian platform, but also within other LIPs around the world.

The Kulumbe (Kulyumber) river area holds the key position in the Siberian Traps province due to its location inside the intermediate zone between the Norilsk-Igarka paleorift zone and the Tunguska syncline. According to the geophysical data, this zone overlays a branch of the Norilsk-Igarka paleorift. The Kulumbe district comprises intrusive complexes both of the northern and southern parts of the Siberian province. Some intrusions with sulfide mineralization are found in this area. The largest Dzhaltul massif is referred to the Kureysky complex. It is important to estimate the place of ore-bearing intrusions in the magmatic evolution of the region in order to find criteria for the rich mineralization prospecting.

Here we present the results of a paleomagnetic and magnetic fabric study of intrusions from the middle reaches of the Kulumbe river. We have also obtained the rare elements data from these intrusions and ore-bearing Dzhaltul massif and compared them with the data from the Norilsk region.

Methods

The paleomagnetic samples were taken as hand blocks oriented using a magnetic compass. Ten to fifteen hand blocks were collected from each site. The local magnetic declination was calculated using the IGRF model (12th generation, revised in 2014). Paleomagnetic research and measurements of the anisotropy of magnetic susceptibility were carried out in the Paleomagnetic laboratory of Schmidt Institute of Physics of the Earth (IPE RAS, Moscow, Russia). All samples were subjected to the stepwise thermal treatment up to the complete demagnetization in 10–17 steps. The majority of samples were demagnetized up to 580–600 °C, in few cases—up to 630 °C. The size of demagnetization steps was changed from 50 to 100 °C at low temperatures to 15–20 °C at high temperatures depending on the

demagnetization pattern. For heating we used MMTD-80 non-magnetic ovens (Magnetic Measurements Ltd, Aughton, U.K.) with internal residual fields of about 5–10 nT. The remanent magnetization of samples was measured using JR-6 spinner magnetometer (AGICO, Brno, Czech Republic) and 2G Enterprises cryogenic magnetometer. Isolation of natural remanent magnetization (NRM) components was performed with Remasoft (Chadima and Hrouda 2006) or Enkin's (1994) paleomagnetic software packages using principal component analysis (Kirschvink 1980). Analysis of paleomagnetic directions was carried out using Fisher statistics (Fisher 1953). Anisotropy of magnetic susceptibility (AMS) was measured by MFK-1FA kappa-bridge (AGICO, Brno, Czech Republic). Processing of the results was performed with Anisoft42 software using Jelinek statistics (Jelinek 1978). Geochemical study of intrusions included determinations of the major components using X-ray fluorescence analysis (Institute of Geology of Ore Deposits, Petrography, Mineralogy and Geochemistry RAS, analyst A. I. Yakushev) and rare elements using the inductively coupled plasma method (ICP-MS, analyst Y. V. Bychkova). In addition, volcanic rocks of the Gudchikhinsky Formation and gabbro of the Talnakh and Dzhaltul intrusions have been analysed.

Geological Background

The study area is located in the middle reaches of the Kulumbe river, 150 km southeast from Norilsk city. The area is situated in the northwestern part of the Siberian platform, at the contact of the Khantaysky-Rybninsky rampart-like uplift and the Tunguska syncline. Ordovician—Lower Carboniferous ($O\text{-}C_1$) carbonate-terrigenous rocks are exposed in the area. Carboniferous deposits of the Tunguska Group overlap the O-C rocks flatly dipping to the east (Fig. 6.1). The main fault structure of this area is the regional Imagda-Letninsky fault of NE strike. The sedimentary rocks are covered by volcanic rocks of the Siberian Traps lava pile ($P_3\text{-}T_1$) representing the southwestern part of the Nirungda Trough.

According to the geological map of Ltd. Norilskgeologiya, the majority of intrusive bodies are referred to as the Katangsky complex, although intrusions of the Kureysky and Ergalakhsky complexes have also been noted. Their diagnostics was carried out in the field conditions only. Meanwhile, their accurate attribution to intrusive complexes is important both for the reconstruction of the magmatic evolution of this area, and for the prospecting of new deposits. New geochemical data on these intrusions are discussed below.

The investigated intrusions are exposed in the Kulumbe river valley and along the creek Khalil (Fig. 6.1). They are mainly located in the sandstones of the Tunguska Group rocks, rarely in the Devonian dolomites referred to as the Nakakhosky Formation. Intrusions usually have sill-like morphology; their thickness varies considerably from the couple of meters to 80–100 m, the visible length is about the first hundreds of meters. Position of intrusions is usually concordant or

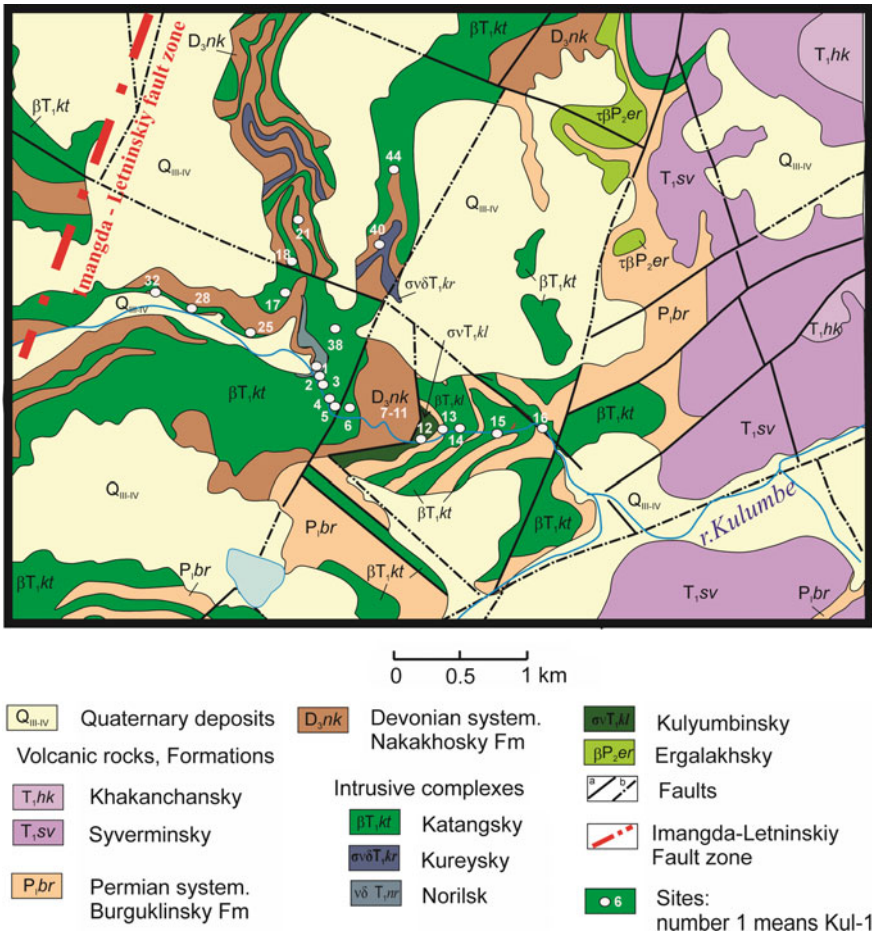

Fig. 6.1 Geological map of the middle reaches of the Kulumbe river valley (after Ltd. Norilskgeologia data with authors' corrections)

sub-concordant with the host rocks which generally form a monocline dipping to the east, with mean dip angles of 10°–15°.

As a rule, intrusive rocks are represented by massive fine-grained gabbro-dolerites without visible differentiation. The exception is the intrusion in site KUL-16 which is characterized by coarse-grained porphyritic texture, where olivine forms large porphyry grains in fine-grained groundmass.

Paleomagnetic Results

We obtained paleomagnetic directions for nine sites from the middle reaches of the Kulumbe river. The quality of the paleomagnetic signal varies from site to site, nevertheless, we were able to calculate the mean directions for all of them. In all sites, we isolated the low-temperature component (LTC) destroyed at 200–300 °C. Since the directions of this component are close to the modern geomagnetic field, we consider that the LTC has a viscous origin. The high-temperature component is also clearly distinguished in all sites. This component is usually destroyed in the temperature range from 350–400 °C to 560−600 °C and decays to the origin (Fig. 6.2a). The directions of this component are close to expected for the Permian-Triassic Siberian Traps (Pavlov et al. 2007, 2015) and we consider it as characteristic. The site-mean directions of the HTC are presented in Table 6.1. Finally, an intermediate middle-temperature component (MTC) occasionally appears in several sites. The temperature range of this component varies from 300 to 500 °C and its directions are scattered. The origin of this component remains unclear.

The HTC in all studied intrusive bodies has the normal polarity except for a single site with the reverse polarity. The concentration parameter K for all directions is slightly higher in the geographic coordinate system than in the stratigraphic system. Moreover, tilt-corrected directions have unusually shallow inclinations compared to those typical for the Siberian Traps. This may imply that the dislocation of the host sedimentary rocks took place before or simultaneously with the

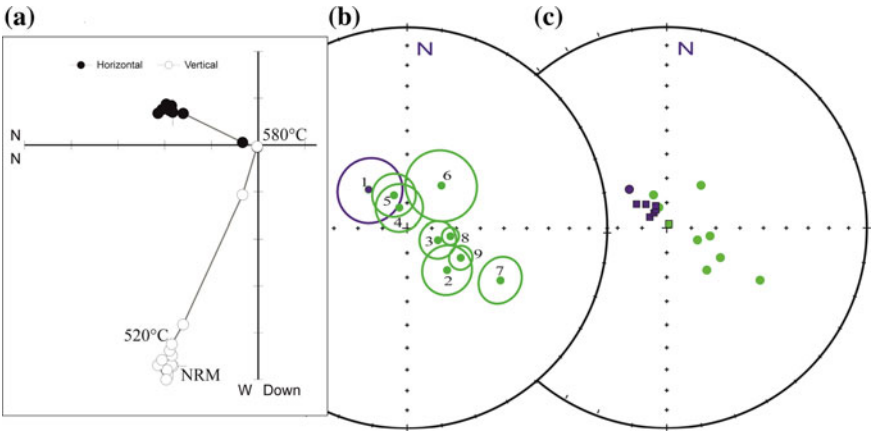

Fig. 6.2 Results of the paleomagnetic investigation. **a**—a typical orthogonal plot for the studied samples. Sample 68, site KUL-14. **b**—site-mean paleomagnetic directions in the geographic coordinate system. Green is normal polarity, blue is reverse polarity. Paleomagnetic sites: 1—KUL-1; 2—KUL-2; 3—KUL-6; 4—KUL-14; 5—KUL-16; 6—KUL-17; 7—KUL-21; 8—KUL-38; 9—KUL-44. **c**—Comparison of our results with the data from Pavlov et al. (2007) which are shown by squares

Table 6.1 The site-mean paleomagnetic directions

Site	N	Dg (°)	Ig (°)	Ds (°)	Is (°)	K	α95
KUL-1	8	314.9	−68.5	301.8	−60.6	18.5	13.2
KUL-2	10	136.4	66.3	124	58	23.9	10.1
KUL-6	14	111.3	76.6	97.9	52.2	29.1	7.5
KUL-14	8	338.5	81.3	39.8	79.5	34.5	9.6
KUL-16	13	337.8	75.8	18.7	76.1	23.2	8.8
KUL-17	13	39.2	67.9	53.6	60.6	9.2	14.5
KUL-21	14	119.2	45.6	115.2	36.7	20.2	9.1
KUL-38	13	100.5	72.1	96.9	62.2	140.5	3.5
KUL-44	14	118.9	65	111.4	55.9	69	4.8
Mean for normal polarity (geographic)	8	99.7	75.6			16.9	13.9
Mean for normal polarity (stratigraphic)	8			95.5	63.6	16.0	14.3

N—number of samples; *Dg*/*Ig*—declination/inclination in situ; *Ds*/*Is*—declination/inclination after tilt correction; K, α95—Fisher statistic parameters

traps emplacement. Our interpretation is consistent with the conclusions of Pavlov et al. (2007) who studied the intrusions in the lower reaches of the Kulumbe river and assumed that the deformations took place at the intermediate stage of the traps emplacement. Therefore, in the discussion below, we consider the site-mean directions in the geographic coordinate system. The distribution of site-mean directions "in situ" is shown in Fig. 6.2b.

The majority of normally magnetized intrusions have steep inclinations, and paleomagnetic directions of the main group are close to those from the upper part of the Norilsk volcanic sequence (the Morongovsky Formation and above; Heunemann et al. 2004). Moreover, the intrusion Norilsk-2 of the Norilsk type also yielded similar direction (Latyshev 2013). According to the geological map of Ltd Norilskgeologiya, the studied intrusions belong to the Katangsky complex widely distributed in the Tunguska syncline.

Site KUL-21 yielded the normal polarity too, but the mean direction is distinct and has significantly shallower inclination (45°) compared to other sites. Such inclinations are unusual for the Siberian Traps and, in the Norilsk region, were reported only for the Syverminsky and Gudchikhinsky Formations from the lower part of the volcanic section (Heunemann et al. 2004; Pavlov et al. 2015). As suggested in these works, this part of the volcanic section was erupted during the reversal of the geomagnetic field within several thousand years and recorded the transitional field state.

Finally, site KUL-1 is the only that yielded the reverse polarity. The site-mean direction is virtually antipodal to that of the main group of normally magnetized intrusions. According to the geological map of Ltd. Norilskgeologiya this intrusion has been referred to as the Katangsky complex as well as the majority of the adjacent sills before, but its paleomagnetic and geochemical (see below) features are distinct.

We compared our results with the data obtained by Pavlov et al. (2007) from the intrusions of the lower reaches of the Kulumbe river. The whole set of site-mean paleomagnetic directions is shown in Fig. 6.2c. As seen from the Figure, the majority of directions reported by Pavlov et al. (2007) has the reverse polarity, in contrast to our data. The reversal test (McFadden and McElhinny 1990) performed for the whole set of site-mean directions is positive: $\gamma/\gamma_{cr} = 8.0°/13.9°$. It argues, firstly, in favor of the primary origin of NRM in studied samples and, secondly, of the averaging of the geomagnetic field secular variations recorded during the intrusions emplacement.

The intrusions sampled by Pavlov et al. (2007) cut Silurian-Devonian sediments, located in deeper horizons of the Siberian platform cover than those studied in this work. Since the normal polarity is predominant in our intrusions, while sills studied by Pavlov et al. (2007) are reversely magnetized (except for one site), we can assume that different magmatic events took place at different levels of the sedimentary cover of the Siberian platform.

AMS Results

We measured the anisotropy of magnetic susceptibility of 15 studied intrusions (Table 6.2). All sites demonstrate the low degree of anisotropy $Pj < 1.035$. The shape parameter T in the majority of sites (11 out of 15) is below zero, corresponding to the prolate shape of AMS ellipsoid. Such values of Pj and T are common for the basic rocks with the primary magmatic magnetic fabric, resulted from the magmatic flow (e.g. Tarling and Hrouda 1993).

Eight sites have so-called normal magnetic fabric, when the minimal axis K3 of AMS ellipsoid is orthogonal to the contact and steep in sills. In this case two other axes K1 and K2 lie in the sill plane and are shallow (Fig. 6.3a). The most common interpretation of the normal magnetic fabric with the low degree of anisotropy is that the magnetic lineation (K1) corresponds to the magma flow direction (Knight and Walker 1988; Tarling and Hrouda 1993; Hrouda et al. 2015). Within all sites with the normal fabric the maximal axes are clustered around the mean shallow axis, and their confidence ellipses do not overlap those of the other axes. Therefore, for the sites with normal magnetic fabric, we interpret the orientation of the maximal axis K1 as the magma flow lineation.

In two other sites, we found the inverse magnetic fabric, when the maximal axis is normal to the contact and steep in sills (Fig. 6.3b). The possible causes of the inversion might be the predominance of single-domain magnetite or titanomagnetite grains (Potter and Stephenson 1988), thermal contraction during the basaltic columns formation (Hrouda et al. 2015) or magnetostatic interaction (Borradaile and Jackson 2010). Within the Siberian Traps province the inverse magnetic fabric was found in sills of the Daldyn-Alakit region (Eastern periphery of the Tunguska syncline) by Konstantinov et al. (2014), who explained the inversion by the contact

Table 6.2 Results of the AMS measurements

Site	Complex	n	Type AMS	Pj	T	K1			K2			K3		
						D	I	Ci	D	I	Ci	D	I	Ci
Kul1	Nr	15	R	1.023	−0.06	49.5	75.2	38.8/22.5	235.9	14.7	48.7/35.7	145.5	1.6	48.8/27.9
Kul2	Kt	8	R	1.023	−0.198	280.0	81.1	17.0/10.8	101.1	8.9	42.2/16.9	11.1	0.2	42.3/10.0
Kul6	Kt	10	N	1.033	0.242	293.6	37.7	43.4/22.3	26.8	4.1	44.4/17.2	122.0	52.0	23.2/21.2
Kul12	Kl	15	S	1.011	−0.100	138.9	52.4	51.7/36.5	355.0	31.9	72.1/50.9	253.5	17.7	72.4/27.2
Kul14	Kt	15	N	1.027	−0.118	309.5	32.0	24.8/10.8	52.7	20.0	31.3/16.4	169.2	50.9	31.4/19.0
Kul16	Kt	16	N	1.022	−0.081	104.4	11.4	38.8/14.0	195.8	6.7	48.5/37.5	315.7	76.7	48.1/11.6
Kul17	Kt	13	S	1.030	−0.123	344.4	7.5	50.5/44.5	81.2	42.1	62.3/48.5	246.3	47.0	62.9/40.2
Kul21	Kl?	11	N	1.017	0.204	273.3	7.5	45.6/28.0	10.3	42.7	62.6/39.5	175.4	46.3	61.5/28.0
Kul24	?	10	N	1.022	−0.115	103.1	5.5	52.9/16.8	194.1	10.5	53.9/26.7	346.0	78.1	32.3/17.4
Kul25	?	15	S	1.023	−0.130	154.9	76.2	83.5/40.7	327.8	13.7	83.6/42.4	58.2	1.6	46.3/41.1
Kul28	?	15	S	1.019	−0.054	357.4	4.7	64.3/40.8	266.1	15.5	65.0/51.6	103.9	73.7	58.5/37.7
Kul32	?	14	N	1.026	0.012	122.7	27.4	21.3/13.0	221.5	16.4	41.3/13.0	338.8	57.3	41.1/20.2
Kul38	Kt	12	N	1.028	0.388	80.0	20.4	34.7/11.9	183.3	31.8	37.1/22.6	322.8	50.8	27.8/10.4
Kul40	?	14	S	1.027	−0.012	39.4	61.2	58.7/36.6	178.6	22.7	76/7/55.7	275.9	16.9	76.6/38.6
Kul44	Kt	9	N	1.028	−0.279	146.7	9.4	13.0/11.2	238.2	8.6	30.5/12.6	9.8	77.2	30.6/10.5

Complex abbreviations: *Kt*—Katangsky, *Nr*—Norilsk, *Kl*—Kulyumbinsky. *n*—number of samples. Types of AMS ellipsoid: *N*—normal, *R*—inverse, *S*—scattered. *Pj*—degree of anisotropy; *T*—shape parameter; *K1*—maximal axis; *K2*—intermediate axis; *K3*—minimal axis. *D*—declination, °; *I*—inclination, °; *Ci*—confidence intervals

influence of the younger intrusions. Thus, additional rock-magnetic and petrographic studies are necessary to solve this problem. Finally, in five sites the dispersed magnetic fabric was observed.

Based on the orientation of the K1 axis in sites with normal magnetic fabric, we determined the predominant lineation of the magma transport. In six out of eight sites, the maximal axis has NW orientation (Fig. 6.3c). This lineation is approximately orthogonal to the regional Imangda-Letninsky fault, which is situated westward from the study area and has NE strike. We suggest that this fault could act as the magma feeding zone during the traps emplacement. This idea is consistent with the results of Callot et al. (2004) who studied the upper part of the volcanic section of the Norilsk region (Morongovsky Formation and above). Based on the AMS measurements, Callot et al. (2004) concluded that the lava eruptions were fed from the rift zone situated in the NW border of the Siberian platform and similar to the regional Norilsk-Kharaelakh fault which is parallel to the Imangda-Letninsky fault and controls the location of the Norilsk ore-bearing intrusions.

Geochemical Data

The study of the intrusions chemical composition shows their clear subdivision into three types (Fig. 6.4). Most of the intrusive bodies have similar geochemical characteristics (Table 6.3). All analyses correspond to gabbro (46.99—51.17 wt% SiO_2) with titanium contents of 1.20–1.56% TiO_2 and sodium predominance over potassium. Porphyritic olivine gabbro from the KUL-16 outcrop are distinguished by higher magnesium content (8.5 wt% MgO), but their other petro- and geochemical characteristics are similar to the other intrusions.

Three types of intrusions can be distinguished from the distribution of rare elements in rocks. The patterns of the main group (Fig. 6.4a) differ by a moderate accumulation of rare elements, clearly negative Ta-Nb and positive Pb and Sr anomalies. These patterns are close to those of the volcanic rocks of the main trap magmatic stage within the Siberian platform, mainly to the Morongovsky-Samoedsky Formations. According to titanium concentrations in the rocks, they could be compared with the Mokulaevsky and Kharaelakhsky Formations. Most of the intrusions belong to the Katangsky complex. Two intrusions have rare elements patterns distinct from the main group (samples KUL-1 and KUL-12—Fig. 6.4b). The first of them has less sharp Ta-Nb anomaly than Katangsky complex intrusions and resembles the rocks of the Norilsk complex [Fig. 6.5a, samples OUG-2/1151.7 and OUG-2/1191 of the Talnakh intrusion; see description and data for intrusions of the Norilsk area in Krivolutskaya (2016)]. Moreover, sulfide mineralization was found in the intrusion KUL-1 (up to 3% sulfides).

However, the most interesting is the sample KUL-12 which is similar to the lavas of the Gudchikhinsky Formation (Fig. 6.5b), which represents the unique example of typical mantle magma in the northwest of the Siberian Traps province (Sobolev et al. 2009). Figure 6.5b shows the spectra for samples of the Gudchikhinsky

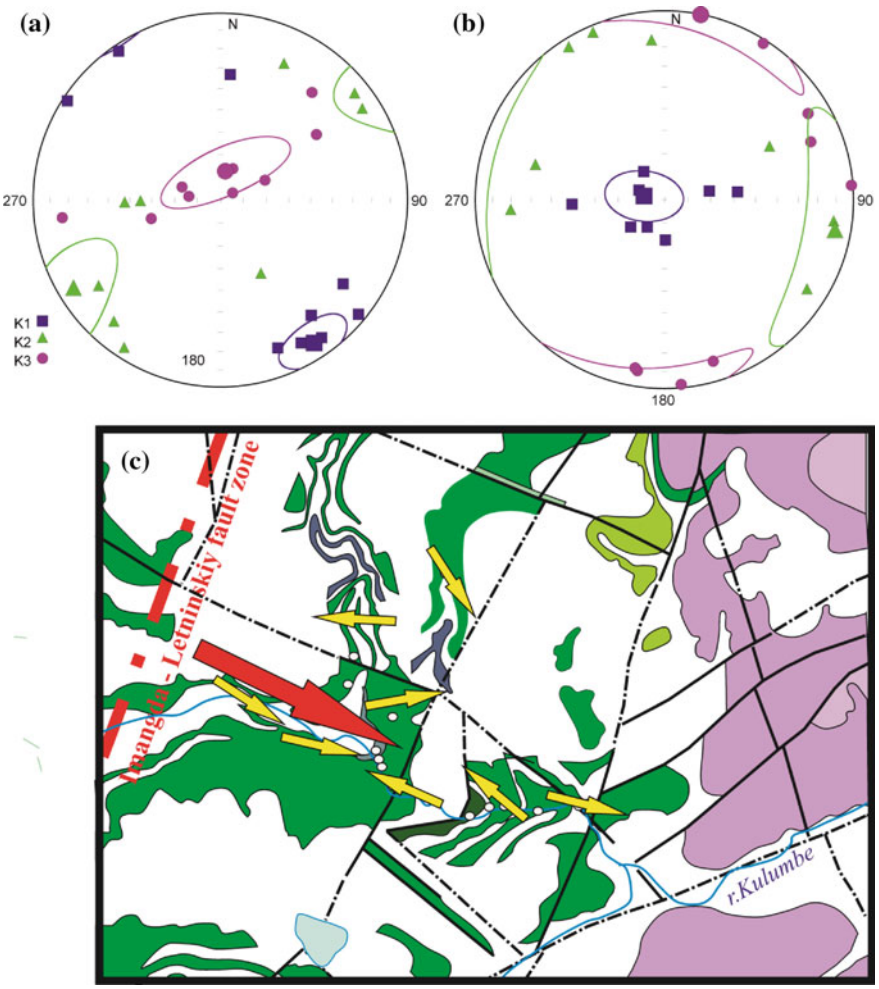

Fig. 6.3 Results of the AMS investigation. **a**–**b**. Examples of the AMS ellipsoid. Geographic coordinate system, equal-area projection. K1—maximal axis; K2—intermediate axis; K3—minimal axis. **A**—site 44, normal magnetic fabric. **b**—site 2, inverse magnetic fabric. **c**—magma flow directions during the intrusions emplacement. Yellow arrows are the site-mean magnetic lineation in the sites with the normal magnetic fabric. Red arrow is the suggested general magma flow direction. Explanatory notes see in caption to Fig. 6.1

Formation taken from the core of borehole OB-36 drilled within the Vologochan Trough in the west of the Norilsk region. These samples have small Ta-Nb and Pb anomalies. Meanwhile, it was demonstrated earlier that the Gudchikhinsky Formation rocks change their composition from west to east, showing the more primitive composition lacking Ta-Nb and Pb anomalies (Sobolev et al. 2009). The spectrum of the KUL-12 sample is similar to these primitive picrites.

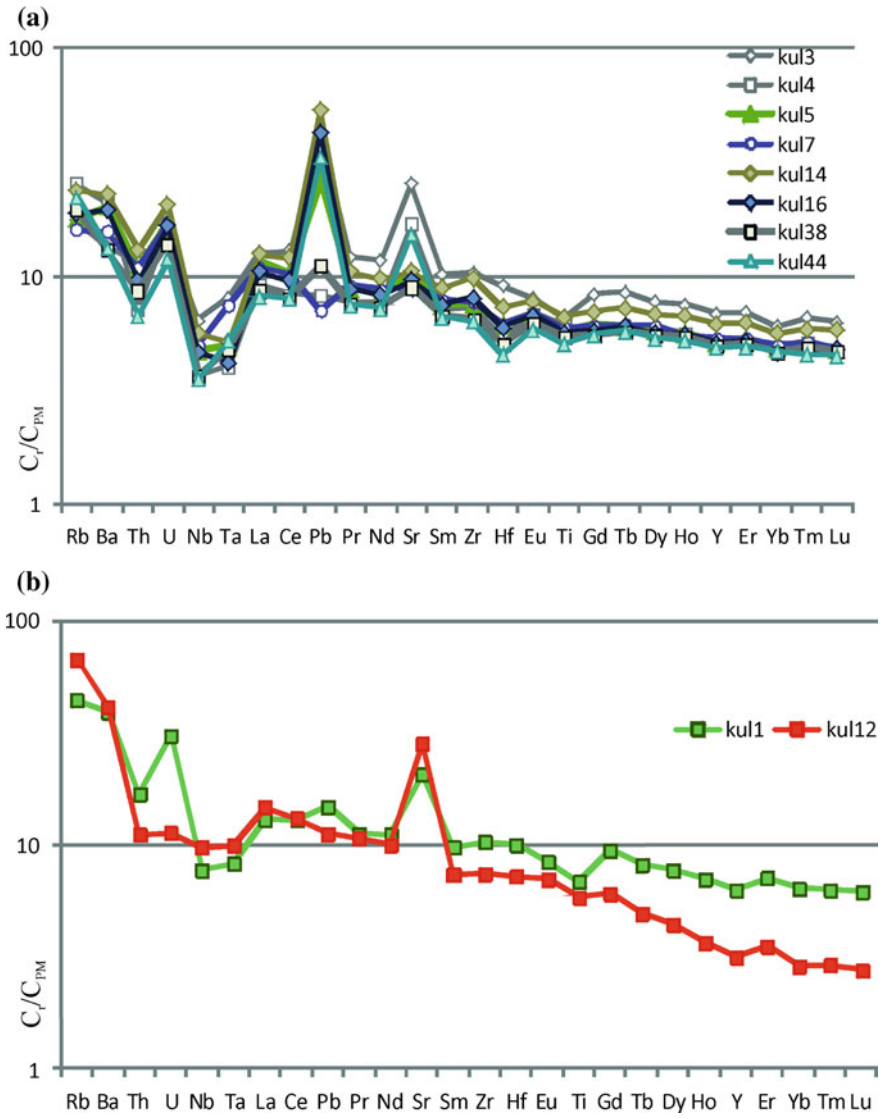

Fig. 6.4 Spider-diagrams for intrusions of the Kulumbe river valley. **a**—Katangsky complex; **b**—other intrusive bodies. Here and in Fig. 6.5 C_r/C_{PM}—content in rock/content in Primitive Mantle (after Hofmann 1988). Data are listed in Table 6.3

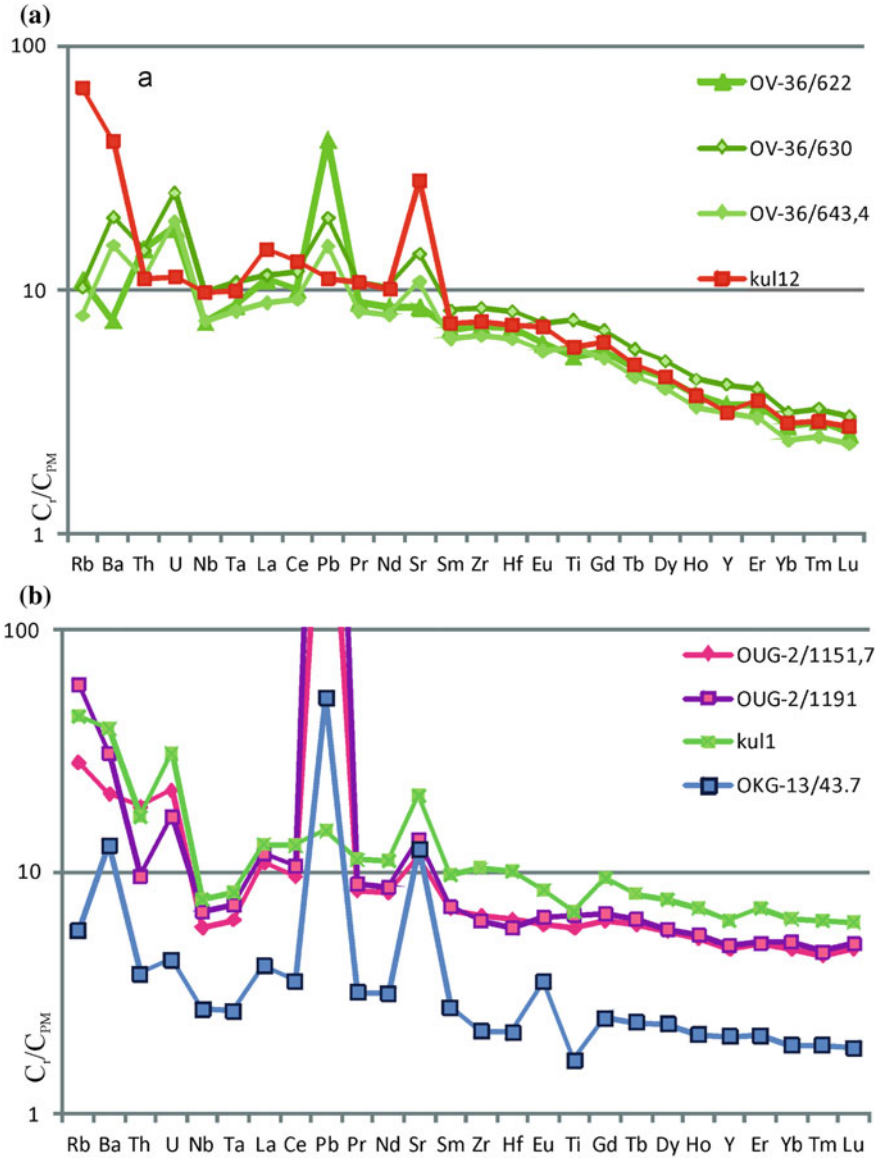

Fig. 6.5 Comparison of spider-diagrams for intrusions and lavas of the Kulumbe river valley and the Norilsk region. Samples, No: OV-36—basalts of the Gudchikhinsky Formation; OUG-2—the Talnakh intrusion (Norilsk complex), OKG-13—Dzhaltul intrusion (Kureysky intrusive complex)

Table 6.3 Chemical composition of the magmatic rocks

N	1	2	3	4	5	6	7	8	9	10	11	12	13	14	15	16
Sample	1151.7	1191	43.7	622	630	643.4	kul3	kul4	kul5	kil7	kul14	kul16	kul38	kul44	kul1	kul12
SiO_2	49.96	49.56	49.66	46.31	48.75	48.25	46.92	46.99	48.18	48.42	48.67	47.59	48.01	48.14	52.17	49.01
TiO_2	1.26	1.42	0.37	1.14	1.62	1.24	1.50	1.43	1.33	1.39	1.56	1.30	1.23	1.20	1.48	1.26
Al_2O_3	14.16	13.35	17.34	8.41	10.77	9.41	14.15	14.21	15.01	14.94	14.69	14.91	15.62	14.98	13.75	14.15
FeO	12.12	12.34	7.59	13.19	13.09	13.17	9.16	13.20	12.88	12.63	13.78	14.11	12.72	9.39	12.87	8.47
MnO	0.21	0.39	0.12	0.18	0.19	0.20	0.12	0.22	0.18	0.17	0.20	0.20	0.18	0.18	0.18	0.11
MgO	7.29	6.73	8.81	19.21	14.47	19.12	6.74	7.34	7.30	7.43	6.23	8.25	7.36	7.27	5.59	6.46
CaO	12.19	11.62	14.02	9.50	9.09	6.98	14.91	9.48	10.04	9.95	10.49	9.99	10.33	11.12	7.18	9.74
Na_2O	2.22	2.84	1.94	1.00	1.17	0.81	3.02	3.50	2.96	2.75	2.59	2.32	2.56	3.53	3.35	2.69
K_2O	0.50	1.06	0.20	0.14	0.11	0.25	0.54	0.69	0.48	0.41	0.56	0.48	0.43	0.57	1.36	1.84
P_2O_5	0.13	0.17	0.03	0.14	0.17	0.14	0.14	0.12	0.14	0.15	0.17	0.14	0.12	0.10	0.15	0.14
LOI							2.49	2.46	1.20	1.55	0.75	0.30	1.18	3.27	1.13	4.81
S	0.01	0.00					0.10	0.13	0.09	0.05	0.08	0.09	0.07	0.04	0.08	0.03
Total	100.07	99.51	100.09	99.23	99.44	99.58	99.79	99.77	99.79	99.84	99.77	99.68	99.81	99.79	99.29	98.72
Rb	17.9	37.9	3.6	6.9	6.5	5.0	11.1	16.1	11.4	10.2	15.1	11.8	12.4	14.0	27.8	42.7
Sr	242	288	262	179	297	228	535	354	220	186	220	202	188	318	434	594
Y	21.7	22.6	9.5	15.4	18.7	14.4	31.2	23.4	23.3	24.5	28.0	23.1	22.7	22.1	28.7	14.4
Ba	147	217	90	52	139	106	94	148	140	109	159	137	91	93	273	285
La	7.47	8.12	2.80	7.55	7.93	6.08	8.73	6.26	8.00	7.46	8.55	7.18	5.87	5.62	8.93	10.13
Ce	16.9	18.8	6.3	17.7	21.1	16.2	23.0	14.8	18.1	18.0	21.3	16.9	14.3	14.1	22.8	23.3
Pr	2.32	2.45	0.87	2.46	2.96	2.27	3.35	2.13	2.45	2.53	2.87	2.42	2.09	2.07	3.09	2.95
Nd	11.2	11.7	4.3	11.6	13.9	10.7	15.8	10.4	11.2	11.9	13.1	11.2	10.0	9.8	15.0	13.6
Sm	3.11	3.19	1.23	3.05	3.67	2.82	4.49	3.18	3.35	3.51	3.94	3.33	3.00	2.94	4.32	3.26
Eu	1.02	1.09	0.59	1.01	1.23	0.94	1.34	1.15	1.16	1.15	1.30	1.14	1.05	0.99	1.41	1.18
Gd	3.77	4.00	1.49	3.35	4.08	3.13	4.97	3.48	3.67	3.62	4.17	3.43	3.27	3.33	5.63	3.63

(continued)

Table 6.3 (continued)

N	1	2	3	4	5	6	7	8	9	10	11	12	13	14	15	16
Tb	0.65	0.69	0.26	0.52	0.62	0.47	0.92	0.64	0.65	0.66	0.78	0.65	0.62	0.62	0.88	0.53
Dy	4.19	4.27	1.73	3.16	3.78	2.90	5.69	4.32	4.30	4.46	5.03	4.14	4.10	3.95	5.69	3.26
Ho	0.87	0.90	0.35	0.61	0.71	0.54	1.23	0.93	0.93	0.91	1.10	0.91	0.89	0.86	1.15	0.60
Er	2.44	2.45	1.01	1.63	1.89	1.45	3.34	2.44	2.56	2.56	3.00	2.50	2.43	2.35	3.39	1.69
Tm	0.33	0.35	0.14	0.21	0.24	0.19	0.49	0.38	0.37	0.38	0.43	0.35	0.36	0.33	0.47	0.21
Yb	2.36	2.52	0.95	1.38	1.55	1.19	2.96	2.42	2.41	2.47	2.76	2.29	2.28	2.31	3.14	1.42
Lu	0.36	0.37	0.14	0.19	0.23	0.17	0.46	0.35	0.36	0.36	0.43	0.36	0.35	0.33	0.46	0.20
Pb	80	2410	3.71	2.91	1.40	1.07	3.02	0.59	1.86	0.50	3.82	3.02	0.79	2.35	1.05	0.79
Th	1.58	0.82	0.32	1.24	1.23	0.95	0.99	0.61	0.93	0.93	1.10	0.81	0.73	0.58	1.43	0.94
U	0.46	0.35	0.09	0.37	0.52	0.40	0.30	0.34	0.36	0.36	0.43	0.35	0.29	0.25	0.65	0.24
Sc	48.1	48.0	42.1	22.7	31.1	23.8	35.1	41.2	35.9	37.4	37.1	31.5	36.2	34.1	36.6	23.7
Ti	7610	8608	2175	6936	9830	7544	8560	7971	7456	7705	8600	7384	7020	6547	8899	7578
V	332	355	224	226	335	257	213	295	262	276	301	250	270	253		
Cr							180	214	151	148	126	119	171	153	149	285
Mn	1794	3323	1101	1522	1817	1394	975	1674	1439	1321	1499	1542	1450	1398	36	21
Co	59	117	53	91	121	93	30	46	47	46	48	56	50	30	69	113
Ni	136	148	304	1058	1296	995	83	132	125	111	99	262	147	109	336	82
Cu	399	4047	361	112	67	51	69	140	115	73	248	659	141	85	62	30
Zn	168	559	52	133	131	100	99	53	70	20	194	47	74	81	20	17
Zr	74	70	25	80	95	73	116	82	85	87	110	90	73	71	116	83
Nb	4.22	4.90	1.93	5.26	6.94	5.33	4.57	2.59	3.34	3.58	4.00	3.30	2.63	2.53	5.51	6.93
Hf	1.97	1.81	0.67	2.18	2.53	1.94	2.79	1.67	1.89	1.91	2.25	1.85	1.56	1.40	3.11	2.23
Ta	0.26	0.30	0.11	0.35	0.44	0.34	0.33	0.17	0.20	0.31	0.21	0.17	0.20	0.22	0.34	0.41

Oxides are given in wt%, elements—in ppm. Empty cell—element was not analyzed. Samples with N = 1–6 are from boreholes (depth in meters is shown in line "sample"): 1–2—OUG-2 (Talnakh intrusion); 3—OKG-13 (Dzhaltul intrusion). 4–6—OV-36 (Gudchikhinsky Formation, basalts)

Discussion

The studied intrusions predominantly belong to the Katangsky intrusive complex which differs from the Norilsk complex by elevated titanium contents and a smaller Ta-Nb anomaly; these intrusions have paleomagnetic directions and geochemical features similar to lavas of the Mokulaevsky-Kharaelakhsky Formations and can be coeval with them. The rocks of the Kureysky complex which was mapped earlier in this area, were not detected (for comparison their geochemical characteristics are given in Table 6.3 and are shown in Fig. 6.5b; see sample OKG-13/43.7 of the Dzhaltul massif of the Kureysky intrusive complex).

For the first time, an intrusive analogue of the rocks of the Gudchikhinsky Formation was discovered. Until now, only the rocks of the Fokinsky massif in the Norilsk region have been compared with the Gudchikhinsky Formation based on high-Mg rock composition. But these rocks were not analyzed using modern geochemical methods, so their comagmatic nature with the Gudchikhinsky rocks was not proved. Besides, the paleomagnetic directions of intrusion KUL-21 point out that its emplacement can be coeval with the Syverminsky-Gudchikhinsky Formations eruption. As the intrusive analogues of the Gudchikhinsky Formation are primarily found in the Kulumbe river valley, we propose to refer to these intrusions as the Kulyumbinsky complex.

KUL-1 intrusion is the only site with the reverse polarity in the studied area and it also differs from other intrusions in the rare element spectra. The geochemical features of sample KUL-1 are similar to those of the Talnakh intrusion.

Our results of the AMS measurements are consistent with the hypothesis of the magma-feeding activity of the regional Imangda-Letninskiy fault of NE strike.

Acknowledgements Authors are very grateful to geologists of Ltd. Norilskgeologia S. Erykalov, V. Rad'ko, V. Sitnikov, A. Lapkovsky, I. Sidorenko and students of Lomonosov Moscow State University M. Nesterenko, D. Korshunov and E. Ostrovsky, Tomsk State University, for their help during the field trip.

This work was funded by RFBR (grants № 16-35-60114, 17-05-01121, 15-05-09250) and the Ministry of Education and Science RF (grant № 14. Z50.31.0017).

References

Borradaile G.J., Jackson M. Structural geology, petrofabric and magnetic fabric (AMS, AARM, AIRM). Journal of Structural Geology, 32 (2010) 1519–1551.

Burgess S.D., Bowring S. A. High-precision geochronology confirms voluminous magmatism before, during, and after Earth's most severe extinction. Science Advances. 2015. Vol. 1, no. 7, e1500470. https://doi.org/10.1126/sciadv.1500470.

Callot J.-P., Gurevitch E., Westphal M., Pozzi J.-P. Flow patterns in the Siberian traps deduced from magnetic fabric studies // Geophys. J. Int. 2004. V. 156. P. 426–430.

Chadima, M., Hrouda, F. 2006. Remasoft 3.0 a user-friendly paleomagnetic data browser and analyzer. Travaux Géophysiques, XXVII, 20–21.

Dobretsov N.L. Permian-Triassic magmatism and sedimentation in Eurasia as reflection of superplume. Doklady Earth Sci. 1997, 354, pp. 220–223.

Enkin R.J. A computer program package for analysis and presentation of paleomagnetic data. Pacific Geoscience Centre, Geological Survey of Canada. 1994. P. 16.

Ernst R.E. Large Igneous Provinces. Cambridge University Press, 2014, 653 p.

Fisher, R. 1953. Dispersion on a Sphere. Proceedings of the Royal Society of London, Series A, Mathematical and Physical Sciences, 217(1130), 295–305.

Heunemann C., Krasa D., Soffel H., Gurevitch E., Bachtadse V. Directions and intensities of the Earth's magnetic field during a reversal: results from the Permo-Triassic Siberian trap basalts, Russia. Earth and Planetary Science Letters. 2004. V. 218. P. 197–213.

Hofmann A. W. Chemical Differentiation of the Earth: Relationship between Mantle, Continental Crust and Oceanic Crust. Earth Planet Sci Lett. 1988. V. 90. pp. 297–314.

Hrouda F., Burianek D., Krejci O., Chadima M. Magnetic fabric and petrology of Miocene sub-volcanic sills and dikes emplaced into the SW Flysch Belt of the West Carpathians (S Moravia, Czech Republic) and their volcanological and tectonic implications. Journal of Volcanology and Geothermal research. 290 (2015) 23–38.

Jelínek, V., 1978. Statistical processing of anisotropy of magnetic susceptibility measures on groups of specimens. Studia geophisica et geodetica 22, 50–62.

Kamo S.L., Czamanske G.K., Amelin Yu. et al. Rapid eruption of Siberian flood-volcanic rocks and evidence for coincidence with the Permian-Triassic boundary and mass extinction at 251 Ma. Earth Planet Sci Lett. 2003. 214, pp. 75–91.

Kirschvink, J.L., 1980. The least-squares line and plane and the analysis of palaeomagnetic data. Geophysical Journal International 62 (3):699–718.

Knight, M.D. & Walker, G.P.L., 1988. Magma flow directions in dikes of the Koolau complex, Oahu, determined from magnetic fabric studies, J. geophys. Res., 93, 4301–4319.

Konstantinov K.M., Mishenin S.G., Tomshin M.D., Kornilova V.P., Kovalchuk O.E. Petromagnetic heterogeneities of the Permo-Triassic traps of the Daldyn-Alakit diamond province (Western Yakutia). Lithosphere. 2014. №2. P. 77–98 (in Russian).

Krivolutskaya N.A. Siberian Traps and Pt-Cu-Ni Deposits in the Noril'sk Area. Springer. 2016. 361 p.

Latyshev A.V. Paleomagnetism of the Siberian Traps: the estimation of the duration and the intensity of magmatic activity in the Norilsk region and Angara-Taseeva depression. PhD thesis. Moscow, 2013 (in Russian).

McFadden P. L., McElhinny M. W. Classification of the reversal test in palaeomagnetism // Geophys. J. Int. 1990. V. 103. P. 725–729.

Pavlov V.E., V. Courtillot, M.L. Bazhenov, R.V. Veselovsky. Paleomagnetism of the Siberian traps: New data and a new overall 250 Ma pole for Siberia. Tectonophysics. V. 443. 2007. pp. 72–92.

Pavlov V., Fluteau F., Veselovskiy R., Fetisova A., Latyshev A., Elkins-Tanton L.T., Sobolev A. V. and N.A. Krivolutskaya (2015). Volcanic pulses in the Siberian Traps as inferred from Permo-Triassic geomagnetic secular variations. Chapter 5 in "Volcanism And Global Environmental Change", A. Schmidt, K.E. Fristad and L. Elkins-Tanton ed., Cambridge University Press, pp. 63–78.

Potter, D.K., Stephenson, A., 1988. Single-domain particles in rocks and magnetic fabric analysis. Geophysical Research Letters, 15, 1097–1100.

Sobolev, A.V., Krivolutskaya N.A., and Kuzmin, D.V. Petrology of the parental melts and mantle sources of Siberian trap magmatism // Petrology, 2009. 17 (3), 253–286.

Tarling, D.H., Hrouda, F., 1993. The Magnetic Anisotropy of Rocks. Chapman, Hall, London, 217 pp.